Structural Evaluation of Cold Region Pavement by FWD Test and its Verification

R. Abe
Civil Engineering Research Institute for Cold Region, Sapporo, Hokkaido, Japan

Y. Kubo
Zukosha Ltd. Sapporo, Hokkaido, Japan

Y. Ozawa
Century-Techno Ltd., Chuo-ku, Tokyo, Japan

K. Matsui
Department of Civil and Environmental Engineering, Tokyo Denki University, Saitama, Japan

ABSTRACT: Mechanistic-empirical pavement design (MEPDG) requires knowledge of material characteristics of pavement layers. Civil Engineering Research Institute for Cold Region has constructed a series of tests at the test sites to establish a MEPDG in a cold region.

Since pavement layer moduli are greatly affected by its surroundings and seasonal changes, FWD tests have been conducted three times a year at the test sites. Pavement is modeled by viscoelastic multilayered half space composed of Voigt model. Layer modulus and damping are identified by the Gauss-Newton method with implementation of wave propagation theory.

The results are confirmed by comparing the computed with measured deflections and also by computed strains and earth pressure with their measured values. Also static backcalculation results are compared with dynamic results. It is found pavement behavior at FWD test can be well explained by using the dynamic backcalculation results.

.

KEY WORDS: FWD, dynamic backcalculation, Young's modulus, damping coefficient, wave propagation, temperature dependency of asphalt concrete

1 INTRODUCTION

Pavement design method under development in many nations has taken a quantum leap from the classical empirical design to mechanistic-empirical design (MEPDG). Mechanistic design requires knowledge of material characteristics of pavement layers. Young's modulus is most important among the characteristics. Since pavement layer moduli are greatly affected by its surroundings and seasonal changes, the best approach to obtain layer Young's moduli is to conduct *in situ* nondestructive testing and estimate their values by using analytical tools such as backcalculation (Dong et al. 2002, Kikuta et al. 1997, Maina et al. 2003, Matsui et al. 2003, Ozawa et al. 2008). Periodical nondestructive tests greatly contribute to establishing a reliable pavement data base which is useful for mechanistic design.

Civil Engineering Research Institute for Cold Region (CERI) has constructed six pavement sections designed by mechanistic approach using elastic multilayered theory in order to establish MEPDG for asphalt pavement in a cold region. They constitute a part of national highway in service located in a northern tip of Japan where it is cold and frozen in winter. Since various hidden dangers are expected in conducting *in situ* tests during the severe winter season, various tests were conducted in June, August and November. The tests include FWD test and measurement of strains and earth pressures. Those data are all taken in time series.

Pavement is composed of viscoelasic layers represented by Voigt model in this study. Young's modulus and damping coefficient of pavement layers are estimated using our dynamic backcalculation software package called Wave BALM (Back Analysis for Layer Moduli). The validity of the results is ascertained from good agreement of computed and measured surface deflections and also by comparing computed strains and earth pressures with their measured values. It is found that the results obtained from dynamic backcalculation coupled with wave propagation explain well not only the surface defections, horizontal strain under asphalt mixture but vertical strain and earth pressure at the top of subgrade.

2 DESCRIPTIONS OF THEORY UTILIZED

2.1 Wave Propagation in Layered Media

Pavement structure assumed in this study is a multilayered half space with layer characteristics of the Voigt model. An impulse force generated by a FWD propagates in the layered system. The wave propagation is expressed by the following equation.

$$\frac{\partial \sigma_r}{\partial r} + \frac{\partial \tau_{rz}}{\partial z} + \frac{\sigma_r - \sigma_\theta}{r} = \rho \frac{\partial^2 u}{\partial t^2} \tag{1a}$$

$$\frac{\partial \tau_{rz}}{\partial r} + \frac{\partial \sigma_z}{\partial z} + \frac{\tau_{rz}}{r} = \rho \frac{\partial^2 w}{\partial t^2} \tag{1b}$$

where u and w are displacement components in the r and z directions, while σ_r, σ_θ, σ_z and τ_{rz} are the components of stress on an infinitesimal axi-symmetric element.

$$\varepsilon_r = \frac{\partial u}{\partial r} \quad , \quad \varepsilon_\theta = \frac{u}{r}, \varepsilon_z = \frac{\partial w}{\partial z}, \gamma_{rz} = \frac{\partial u}{\partial z} + \frac{\partial w}{\partial r} \tag{2}$$

$\varepsilon_r, \varepsilon_\theta$ and ε_z are normal strains in r, θ and z directions and γ_{rz} is a shearing strain. The stress-strain relationship described by Voigt model(Figure 1) are given as,

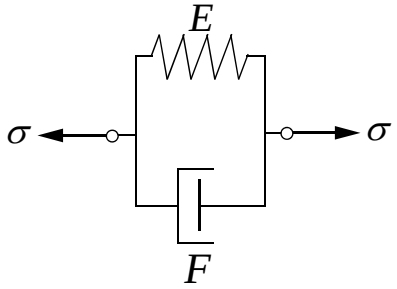

Figure 1: Voigt Model

$$\begin{Bmatrix}\sigma_r\\ \sigma_\theta\\ \sigma_z\\ \tau_{rz}\end{Bmatrix}=\left(E+F\frac{d}{dt}\right)\begin{pmatrix}b+2c & b & b & 0\\ b & b+2c & b & 0\\ b & b & b+2c & 0\\ 0 & 0 & 0 & c\end{pmatrix}\begin{Bmatrix}\varepsilon_r\\ \varepsilon_\theta\\ \varepsilon_z\\ \gamma_{rz}\end{Bmatrix} \tag{3}$$

where

$$b=\frac{\nu}{(1+\nu)(1-2\nu)}\quad,\quad c=\frac{1}{2(1+\nu)}$$

E is Young's modulus, F is damping coefficient and ν is Poisson's ratio.

In case of multilayered system such as pavement, material property and thickness of each layer may differ, the relationship of Equations (1)-(3) holds at all layers. When an impulsive force acts at the surface of multilayered system, the boundary conditions at the surface can be given as,

$$\sigma_z(r,0,t)=-p(t) \qquad |r|\le a \tag{4a}$$

$$=0 \qquad |r|>a \tag{4b}$$

$$\tau_{rz}(r,0,t)=0 \qquad r\ge 0 \tag{4c}$$

in which,

$$p(t)=P(t)/\left(\pi a^2\right) \tag{4d}$$

The solution of Equations (1)-(4) can be obtained using Hankel transform and FFT (Fast Fourier Transform). The solution procedure is described in Reference (Ozawa and Matsui, 2008).

2.2 Backcalculation

This study estimates layer modulus E_j and damping coefficient F_j of pavement from histories of impulse force and deflections of several points at the surface, assuming pavement layers are described by Voigt model. The subscript $j(=1,...,M)$ denotes layer number. The unknowns E_j and F_j are determined such that measured deflections $w_i(t)$ agrees with computed deflections $z_i(E_j,F_j,t)$ at sensor i $(i=1,...,N)$.

Backcalculation is a nonlinear least square problem which requires an iterative computation to solve it. One computes surface deflections at FWD sensor locations assuming the seed values of $\mathbf{X}=\left(E_j,F_j\right)^T$, and the square sum of difference between measured and computed deflections at discrete time points are minimized to estimate the unknown parameters. The objective function is defined as,

$$J=\frac{1}{2}\sum_{i=1}^{N}\sum_{k=1}^{K}\left\{w_i(t_k)-z_i(\mathbf{X},t_k)\right\}^2 \tag{5}$$

where

$w_i(t_k)$: measured deflection at sensor i at time step t_k.

$z_i(\mathbf{X},t_k)$: computed deflection at sensor i at time step t_k.

$\mathbf{X}$: a vector composed of unknown parameters (layer modulus and layer damping).

N : number of point of interest.
K : number of discrete time steps in the matching interval.

The time interval which measured and computed deflections are compared is defined as $t_0 \le t \le t_1$. t_0 is the time step at which the deflection at the center of load has exceeded 50% of its peak deflection and , t_1 is the time step at which the deflection at the furthest sensor has reduced beyond 50% of its peak.

Gauss Newton method coupled with truncated singular value decomposition is employed (Ozawa et al. 2008). From the necessary condition for Equation (5) becomes minimum, one will obtain,

$$\sum_{j=1}^{2M}\sum_{k=1}^{K}\left\{\sum_{i=1}^{N}\frac{\partial z_i(\mathbf{X},t_k)}{\partial X_\ell}\frac{\partial z_i(\mathbf{X},t_k)}{\partial X_j}\right\}dX_j = \sum_{k=1}^{K}\sum_{i=1}^{N}\left(w_i(t_k)-z_i(\mathbf{X},t_k)\right)\frac{\partial z_i}{\partial X_\ell} \qquad (6)$$
$$\ell = 1,\ldots,2M$$

Equation (6) is a system of $2M \times 2M$ simultaneous equations. Because the condition number of coefficient matrix often becomes very large and the matrix approaches to a singular matrix, it must be solved with a great care. Goodness of fit is evaluated by the following,

$$E_r = \sqrt{\frac{\sum_{i=1}^{N}\sum_{k=1}^{K}\{w_i(t_k)-z_i(\mathbf{X},t_k)\}^2}{N\cdot K}} \qquad (7)$$

3 DESCRIPTIONS OF TEST SITES AND FWD TESTS

3.1 Test Sites

Six test pavement sections are constructed as a part of national highway in the city of Wakkanai, Hokkaido. Daily traffic volume of heavy vehicles at the test site is from 1000 to 3000. Their profiles are given in Table 1. Composition of asphalt mixture is explained below the table. Soft rock (mudstone) layer underlies from 2 m to 3m below the pavement surface. The top of the soft rock is likely to be rugged.

Table 1: Pavement profile (cm)

	Section 1	Section 2	Section 3	Section 4	Section 5	Section 6
AC mixtures	10.7	11.1	16	23	32.3	32.5
Base	77.3	70.9	100	62.6	52.7	51.5
Subgrade	210	190	275	200	154	140

Section 1: surface course and bituminous stabilized layer
Section 2: surface course and dense asphalt concrete
Section 3: surface course, intermediate layer and bituminous stabilized layer
Section 4: surface course, intermediate layer, binder course and dense asphalt concrete
Section 5: surface course, intermediate layer, binder course and bituminous stabilized layer
Section 6: surface course, intermediate layer, binder course and bituminous stabilized layer

Test sections 1, 2, 5 and 6 were completed in the fall of 2003 and Section 3 and 4 were constructed in the fall of 2005. At the construction in 2005, strain gages were laid at the bottom of asphalt mixture, strain gages and earth pressure cells at the top of subgrade of not only Section 3 but Sections 1 and 6. Sensor placed parts of Sections 1 and 6 are called Section 1-2 and Section 6-2, while the part without sensors called Section 1-1 and Section 6-1 respectively. The number of sections where FWD tests were conducted is 8 sections all together. At the constructions stage, thermocouples were also placed in layers of asphalt mixture with which pavement temperatures have been monitored.

3.2 FWD Tests

FWD test has been conducted at 8 sections which include from Section 1 to Section 6 and two extra sections called Section 1-2 and 6-2 where strain gages and earth pressure cell were laid in the fall of 2005. Test locations at each section were illustrated in Figure 2. FWD test was conducted in June, August and November.

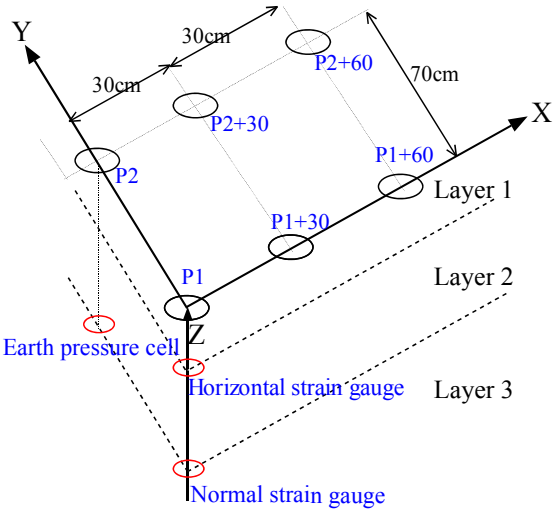

Figure 2 Locations of FWD test and locations of strain gages and earth pressure cell

4 BACKCALCULATION RESULTS

4.1 Layer Modulus and Layer Damping

FWD tests were carried out at six locations of eight sections in June, August and November. Backcalculation was executed using Wave BALM. At Sections 1-2, 3 and 6-2, static backcalculation was also made using the peak values of load and responses. Backcalculation is known in general computationally unstable. Thus 50 sets of seed values are randomly generated in the following ranges $E_1 = 1000\text{MPa} - 10{,}000\text{MPa}$, $E_2 = 100\text{MPa} - 500\text{MPa}$, $E_3 = 50\text{MPa} - 150\text{MPa}$, $E_4 = 100\text{MPa} - 1000\text{MPa}$. Seed values of layer damping coefficient are taken as 1 % of seed values of layer modulus.

Mean layer modulus, damping coefficient and their standard of variations estimated from FWD data at P1-0 are tabulated in Table 2. In the table, the results of static backcalculation using peak load and peak deflections are also described.

The table shows that layer modulus of asphalt mixture is lower in August than that in November. It manifests temperature dependency of asphalt mixture. The backcalculated results show that the standard deviation of the lowest soft rock modulus is larger than other layers. It implies that if a stiff layer exists below 2 meters under the less stiff layer, estimation of the lowest layer seems difficult. Judging from great difference in the mean values of soft rock, the modulus is not uniform in all sections tested. The ratio of damping coefficient over modulus of layer is from 1% to 3% in asphalt mixture and from 0.2% to 1% in base course and subgrade.

Table 2: Backcalculated results

			June				August				November			
			Young's Modulus		Damping cofficient		Young's Modulus		Damping cofficient		Young's Modulus		Damping cofficient	
			Result	Standard Deviation	Result	Standard Deviation	Result	Standard Deviation	Result	Standard Deviation	Result	Standard Deviation	Result	Standard Deviation
Unit			MPa	MPa	MPa・s	MPa・s	MPa	MPa	MPa・s	MPa・s	MPa	MPa	MPa・s	MPa・s
Section 1-1	Layer 1		649	13.78	17.13	0.09	997	25.39	26.20	0.15	2649	33.92	38.20	0.17
	Layer 2		127	0.85	0.33	0.01	121	1.13	0.28	0.01	116	1.03	0.28	0.01
	Layer 3		118	7.45	0.69	0.01	112	8.60	0.70	0.01	118	5.55	0.54	0.01
	Layer 4		53	10.02	1.49	0.50	56	12.23	2.14	0.69	39	7.59	1.21	0.32
Section 1-2	Layer 1	Weve BALM	1347	49.84	25.64	0.23	781	23.42	18.26	0.35	3260	58.52	32.82	0.83
		BALM	3031	42.74	-	-	1924	21.64	-	-	5102	456.48	-	-
	Layer 2	Weve BALM	86	1.73	0.20	0.01	88	1.09	0.21	0.01	78	1.50	0.23	0.02
		BALM	90	1.40	-	-	95	1.24	-	-	84	7.26	-	-
	Layer 3	Weve BALM	104	14.65	0.63	0.00	80	15.83	1.04	0.08	114	11.38	0.35	0.05
		BALM	106	10.13	-	-	113	11.44	-	-	93	12.29	-	-
	Layer 4	Weve BALM	197	111.95	2.25	1.42	211	115.11	2.10	1.36	191	110.26	2.38	1.29
		BALM	641	242.00	-	-	581	234.24	-	-	691	257.11	-	-
Section 2	Layer 1		1236	89.86	29.21	3.87	656	68.97	18.31	2.15	4855	139.34	66.11	0.68
	Layer 2		145	1.08	0.30	0.13	146	1.29	0.33	0.11	138	3.56	0.23	0.02
	Layer 3		110	29.03	0.76	0.34	110	30.84	0.84	0.33	147	14.14	0.56	0.02
	Layer 4		403	164.19	3.14	0.76	415	116.10	2.59	0.76	39	10.54	1.30	0.38
Section 3	Layer 1	Weve BALM	2502	140.77	37.12	1.03	1162	90.07	22.62	0.81	9078	348.62	63.37	1.30
		BALM	4018	146.23	-	-	2308	24.81	-	-	9287	2401.22	-	-
	Layer 2	Weve BALM	94	3.63	0.30	0.02	93	3.18	0.31	0.02	81	5.09	0.33	0.02
		BALM	117	4.55	-	-	110	2.00	-	-	147	50.18	-	-
	Layer 3	Weve BALM	83	4.10	0.17	0.08	91	4.03	0.21	0.10	108	7.70	0.17	0.07
		BALM	68	7.05	-	-	76	8.40	-	-	67	16.17	-	-
	Layer 4	Weve BALM	699	229.21	2.15	1.01	500	191.77	2.24	1.20	517	218.00	2.15	0.98
		BALM	460	167.74	-	-	467	187.81	-	-	525	176.64	-	-
Section 4	Layer 1		1062	1.21	17.84	0.06	867	1.53	15.21	0.05	3337	4.29	27.09	0.27
	Layer 2		114	0.47	0.29	0.00	105	0.51	0.30	0.00	146	0.69	0.49	0.01
	Layer 3		99	0.86	0.17	0.00	108	1.08	0.20	0.00	84	0.72	0.17	0.00
	Layer 4		17	1.27	0.88	0.05	16	1.05	0.73	0.04	30	2.17	2.19	0.19
Section 5	Layer 1		1785	2.17	17.94	0.15	586	0.48	11.05	0.02	5345	60.31	18.81	1.31
	Layer 2		193	1.03	0.66	0.04	177	0.27	0.52	0.01	166	6.94	1.55	0.07
	Layer 3		88	0.77	0.31	0.01	138	0.56	0.16	0.00	71	4.96	0.29	0.02
	Layer 4		83	6.38	4.83	0.29	25	1.80	1.13	0.02	488	129.45	11.95	3.22
Section 6-1	Layer 1		1566	9.58	15.39	0.10	1546	7.15	15.47	0.09	6131	82.24	27.82	1.27
	Layer 2		65	2.30	0.60	0.01	61	1.56	0.58	0.01	89	3.75	0.75	0.01
	Layer 3		105	2.88	0.17	0.01	105	2.64	0.17	0.01	78	2.16	0.13	0.01
	Layer 4		726	163.84	33.76	6.78	682	141.44	35.50	8.41	1870	557.82	3.59	2.79
Section 6-2	Layer 1	Weve BALM	2002	42.07	17.46	0.35	1581	27.55	15.14	0.19	5978	110.94	28.30	1.45
		BALM	2865	80.95	-	-	2313	60.36	-	-	7270	402.98	-	-
	Layer 2	Weve BALM	50	5.76	0.31	0.03	49	3.71	0.30	0.02	111	19.09	0.55	0.09
		BALM	74	12.39	-	-	70	10.45	-	-	149	43.84	-	-
	Layer 3	Weve BALM	132	27.99	0.45	0.10	134	21.27	0.39	0.09	87	11.10	0.19	0.06
		BALM	105	19.28	-	-	103	19.63	-	-	72	14.84	-	-
	Layer 4	Weve BALM	1332	783.57	8.06	4.43	1354	818.87	8.01	4.29	1034	389.35	2.81	1.18
		BALM	922	366.79	-	-	918	358.58	-	-	713	262.31	-	-

4.2 Comparison of Measured and Computed Responses

Figure 2 shows the location of strain gages and earth pressure cell of Section 1-2, Section 3 and Section 6-2. Horizontal strain is measured under asphalt mixture layer and vertical strain at the top of subgrade below P1-0, and vertical stresses at the top of subgrade under P2-0. Figures 3 illustrates the comparison of measured and computed responses: surface deflections,

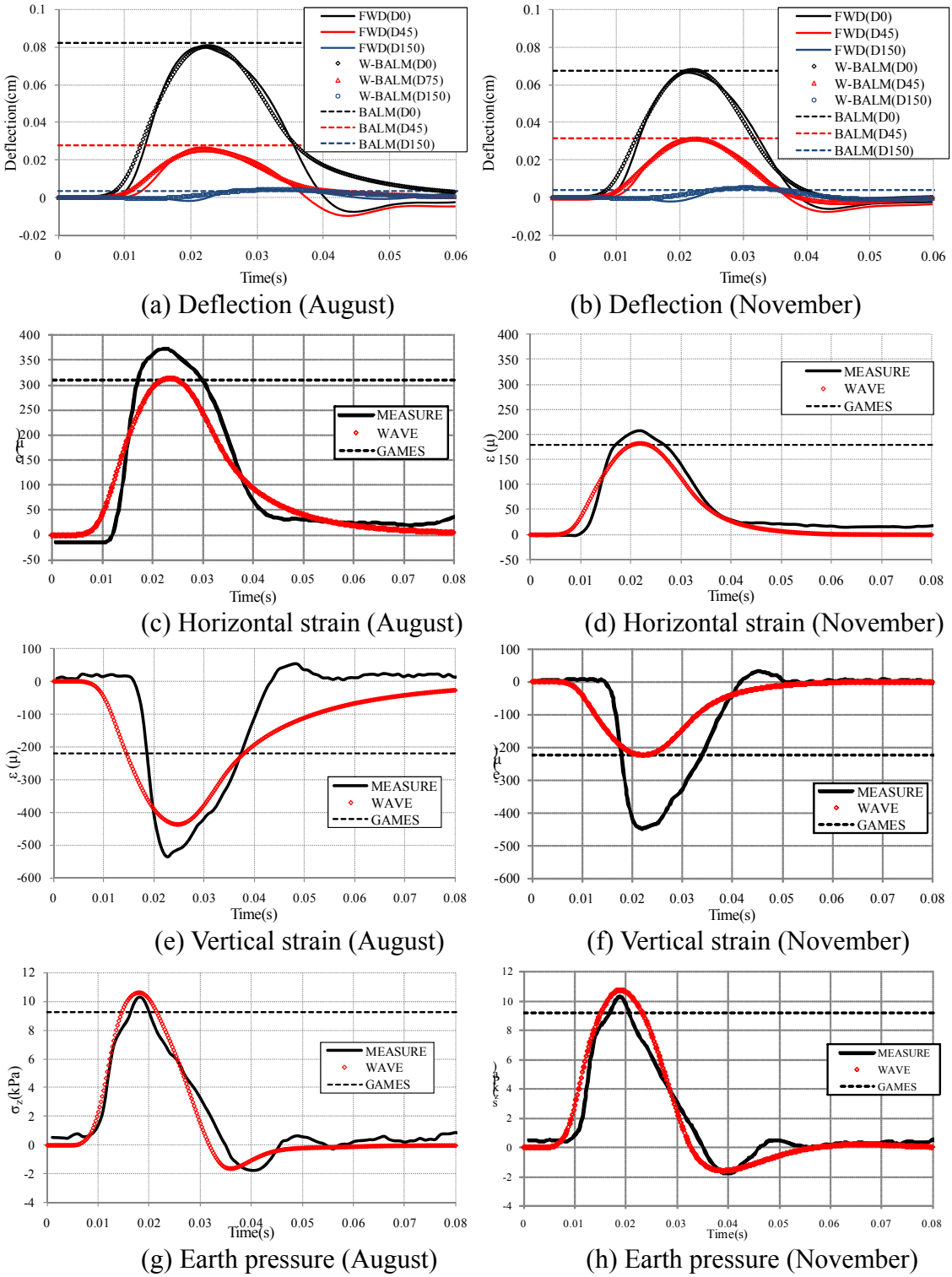

Figure 3: Comparison of responses at Section 1-2

horizontal strains, vertical strains and vertical pressures. The surface deflections are compared only at the center of load, 45 cm and 150 cm off from the center in August and November respectively. In the figures the broken lines indicate the results from static backcalculation. The computed surface deflections manifest an excellent agreement with the measured ones in the both figures.

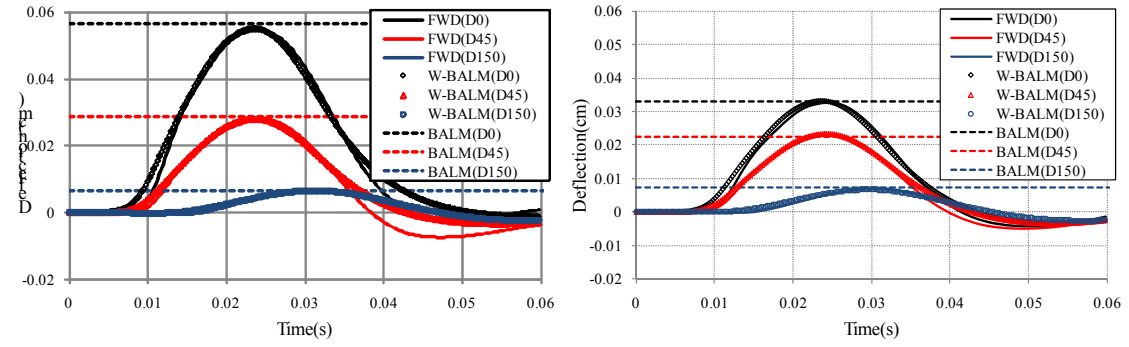

(a) Deflection (August) (b) Deflection (November)

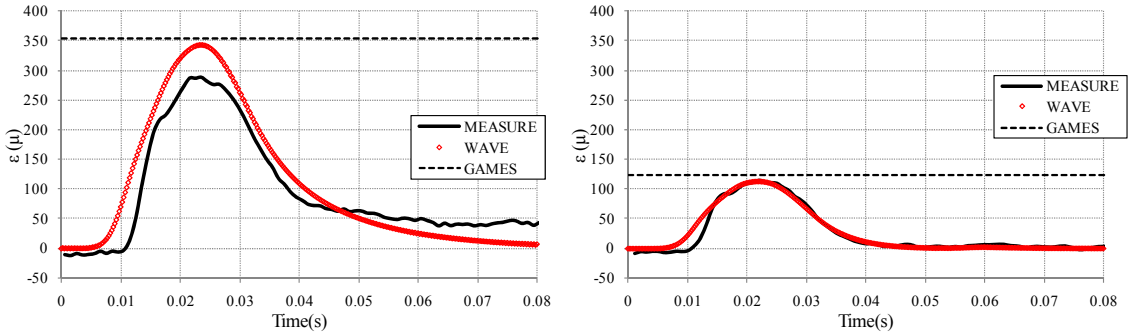

(c) Horizontal strain (August) (d) Horizontal strain (November)

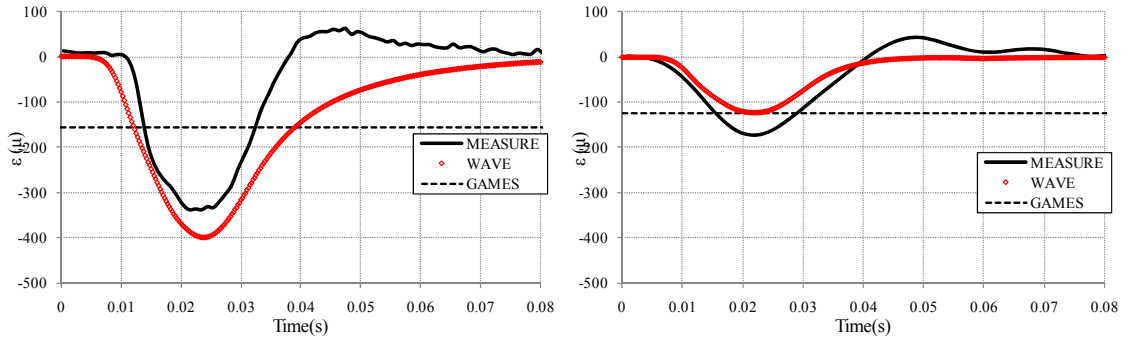

(e) Vertical strain (August) (f) Vertical strain (November)

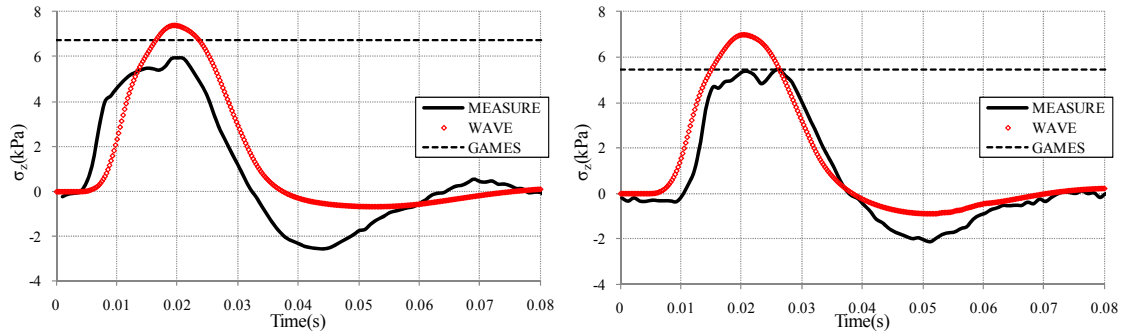

(g) Earth pressure (August) (h) Earth pressure (November)

Figure 4: Comparisons of responses at Section 3

Figures 3(c) and 3(d) describe the comparison of measured and computed horizontal strains at the bottoms of asphalt mixture in August and in November respectively. Though the computed strains are little smaller than the measured strains, both strains show good agreement. The strain obtained from static backcalculation shows good agreement with peak strain. Figures 3(e) and 3(f) compare the measured and computed vertical strains at the tops of subgrade. Difference between measured and computed strains is small in August, while the difference is relatively large in November. The subgrade modulus from static backcalculation tends to results in larger estimate than dynamic backcalculation does. It seems this is why the vertical strain at the top of subgrade becomes much smaller than the measured strain. The peak strains in August and November are about 500μ, which may be still considered linear (Goto *et al*. 1999). Figures 3(g) and 3(h) compare the measured and computed vertical pressure at the top of subgrade. Measured and computed vertical pressures agree quite well for both dynamic and static analyses.

Figure 4 shows the comparisons of measured and computed results obtained from FWD tests conducted at P1-0 of Section 3 in August and in November. The results obtained FWD tests are very much similar with the results of Section 1-2.

5. RELATIONSHIP BETWEEN MODULUS AND TEMPERATURE OF ASPHALT COMPOSITES

It is well known that stiffness of asphalt mixture depends on its temperature. The model is assumed as,

$$E(T) = \frac{E_\infty}{1+10^{\alpha T+\beta}} \tag{8}$$

E_∞ means the modulus of asphalt mixture when temperature approaches $-\infty$ in which α and β are unknown parameters and must be determined from backcalculated results. Since there is no data available for stiffness of asphalt mixture at very low temperature, it is difficult to estimate the value of E_∞. From empirical knowledge, the stiffness is assumes as $E_\infty = 30000$MPa the parameter values of α and β are found as $\alpha = 0.042, \beta = 0.223$.

Plots of backcalculated modulus vs. temperature are drawn with Equation 8 in Figure 5. Backcalculated results of Section 3 look different from others. The reason is not known but it is presumed that the depth to underlying soft rock greatly varies.

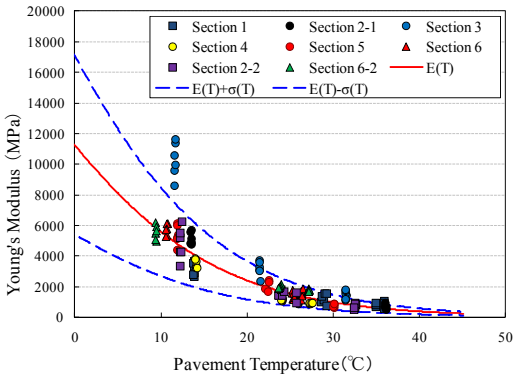

Figure 5: Backcalculated layer moduli vs pavement temperature

6 CONCLUSIONS

Pavement is assumed as viscoelasitc multilayered half space composed of Voigt model. This study estimates layer modulus and damping coefficient in the model by backcalculating FWD time series data. By using backcalculated results, computed strains and vertical stresses are compared with measured values.

From Table 2:

1) Layer modulus of soft rock lying around more than 2 m below pavement surface is difficult to estimate with good accuracy.
2) It is confirmed that layer modulus of asphalt concrete greatly changes depending on its temperature.
3) Damping coefficient in asphalt mixture is from 1% to 3% and those in base and subgrade are from 0.2 % to 1% of their corresponding moduli.

From Figure 3 to Figure 4:

4) Computed surface deflections demonstrate excellent agreement with measured deflections.
5) Computed horizontal strains at the bottom of asphalt mixtures match well with measured strains.
6) Static and peak dynamic stains are close to each other.
7) Computed dynamic vertical strains at the top of subgrade can simulate measured strains. However static strains are quite different from peak measured deflections.
8) Computed earth pressure at the top of subgrade shows relatively good agreement.

From Figure 5:

9) Excluding asphalt mixture of Section 3, the relationship between asphalt mixtures and its mean temperature can be expressed as $E(T) = 30{,}000 \Big/ \left(1 + 10^{0.042T + 0.223}\right)$

The comparison of computed responses with measured responses makes clear that the wave propagation based backcalculation method is found useful tool to examine the characteristics of pavement structures.

REFERENCES

Dong, Q. X., Matsui, K., Hachiya, Y., and Tsubokawa, Y., 2003. *Efficient finite element and sensitivity analyses of elastic multi-layered systems subject to an impulsive force.* JSCE, No. 731/I-63: 247-255. (in Japanese)

Goto, S., Burland, J.B. and Tatsuoka, F. 1999. *Nonlinear soil models at various strain levels and its application to axisymmetric excavation problem*, Soils and Foundations, Japanese Geotechnical Society, Vol. 39, No. 4, 111-119, Aug. 1999.

Kikuta, Y., Matsui, K., Enya, T., Abe, Y., 1997. *Time domain backcalculation of pavement structure by using matrix reduction.* JSCE, No.557/V-34: 77-85. Japan. (in Japanese).

Maina, J. W., Matsui, K. Kikuta, Y. and Inoue, T. 2004. *Dynamic Backcalculation of Pavement Structure using Multiple Sets of Time Series data.* Geo Institute Conference on Geotechnical Engineering for Transportation Projects. USA.

Matsui, K., Maina, J. W., Dong, Q., and Sasaki, Y. 2003. *A fast dynamic backcalculation of layer moduli using axi-symmetric approach*. International Journal of Pavements (IJP), Volume 2, Number 1-2. 75-87. USA.

Ozawa, Y. and Matsui K. 2008, Wave propagation analysis of pavement structures composed of Voigt model, Journal of JSCE, Division E, Vol.64 No.2, pp.314-322. (in Japanese)

Ozawa, Y., Shinohara, Y., Matsui, K., and Higashi, S., 2008., *Structural evaluation of multilayered viscoelastic media using wave propagation theory*, Journal of JSCE, Division E, Vol.64 No.4, pp.533-540. (in Japanese)